

Enhanced quantum oscillatory magnetization and nonequilibrium currents in an interacting two-dimensional electron system in MgZnO/ZnO with repulsive scatterers

M. Brasse,¹ S. M. Sauther,¹ J. Falson,² Y. Kozuka,² A. Tsukazaki,³ Ch. Heyn,⁴ M. A. Wilde,^{1,*} M. Kawasaki,² and D. Grundler¹

¹*Lehrstuhl für Physik funktionaler Schichtsysteme, Physik-Department, Technische Universität München, 85748 Garching, Germany*

²*Department of Applied Physics and Quantum-Phase Electronics Center (QPEC), University of Tokyo, Tokyo 113-8656, Japan*

³*Institute for Materials Research, Tohoku University, Sendai 980-8577, Japan, and PRESTO, Japan Science and Technology Agency (JST), Tokyo 102-0075, Japan*

⁴*Institut für Angewandte Physik, Universität Hamburg, Jungiusstrasse 11, 20355 Hamburg, Germany*

(Received 15 July 2013; published 18 February 2014)

Torque magnetometry at low temperature and in high magnetic fields B is performed on MgZnO/ZnO heterostructures incorporating high-mobility two-dimensional electron systems. We find a sawtoothlike quantum oscillatory magnetization $M(B)$, i.e., the de Haas-van Alphen (dHvA) effect. At the same time, nonequilibrium currents and unexpected spikelike overshoots in M are observed which allow us to identify the microscopic nature and density of the residual disorder. The acceptorlike scatterers give rise to a magnetic thaw down effect which enhances the dHvA amplitude beyond the electron-electron interaction effects being present in the MgZnO/ZnO heterostructures.

DOI: [10.1103/PhysRevB.89.075307](https://doi.org/10.1103/PhysRevB.89.075307)

PACS number(s): 71.18.+y, 77.55.hf, 71.70.-d

Two-dimensional electron systems (2DESs) formed in oxide heterostructures without intentional doping have generated tremendous interest in recent years [1,2] and exhibit remarkable properties, such as superconductivity [3], magnetism [4], or the fractional quantum Hall effect (QHE) [5,6]. MgZnO/ZnO-based heterostructures are outstanding in that 2DESs of small carrier density n_s exhibit extremely high mobilities μ at low temperature T [5,6]. At the same time, the electron-electron interaction parameter $r_s \propto n_s^{-0.5}$ [7] is large, allowing for strong electronic correlation effects as compared to conventional III-V semiconductor 2DESs [6,8,9]. Still, the quantum oscillatory magnetization $M(B)$, i.e., the de Haas-van Alphen (dHvA) effect, reflecting the ground state properties of 2DESs has not yet been explored. Since the discovery of the dHvA effect in Bi more than eight decades ago, it has been argued that disorder *reduces* the peak-to-peak amplitudes ΔM via broadening of the quantized Landau levels E_j ($j = 0, 1, 2, \dots$) [10–12]. In contrast, electron-electron interaction effects are known to enhance ΔM [13]. The two counteracting effects are, however, not easy to distinguish in a balancing situation. Sometimes the dHvA effect has been obscured in the QHE regime by large nonequilibrium currents (NECs) [14,15]. The NECs are induced near integer filling factors $\nu = hn_s/(eB_\perp)$ at low T when the longitudinal resistivity ρ_{xx} takes a vanishingly small value and are believed to be limited only by the breakdown of the QHE [15]. Independent transport experiments on GaAs-based heterostructures have evidenced that, strikingly, minima in ρ_{xx} and plateaus in the Hall resistivity ρ_{xy} could be displaced away from integer ν towards smaller ν due to repulsive scatterers [16–20]. This phenomenon has not yet been resolved in $M(B)$, and an experimental manifestation of the underlying asymmetric density of states (DOS) in a ground state property is lacking.

In this paper, we report torque magnetometry on the equilibrium dHvA effect and NECs of a high-mobility 2DES

residing at a MgZnO/ZnO heterointerface. We observe dHvA amplitudes ΔM at $\nu = 1$ and 2 that are significantly enhanced over the values expected in the single-particle picture. Addressing a regime $0.28 \text{ K} < T < 1.6 \text{ K}$ we observe T -dependent shifts of both the dHvA effect and the NECs. At the same time, spikelike overshoots of the equilibrium magnetization are found near $\nu = 1$ and 2. These unforeseen characteristics of M are consistently attributed to a disorder-induced asymmetric DOS due to short range repulsive scatterers and the magnetic thaw down of electrons in magnetoacceptor (MA) states [17,19,20]. Contrary to the orthodox thinking, the disorder in MgZnO/ZnO is found to provoke, thereby, an *increase* of the equilibrium magnetization near integer ν instead of the anticipated reduction. In particular, $M(B)$ allows us to quantify the density of MA states which is important to further optimize MgZnO/ZnO heterostructures for basic research and technological applications. The discovery of unintentional repulsive short range scatterers is of special significance in MgZnO/ZnO since the 2DES is formed without any intentional doping, meaning that the remote-donor scattering unavoidable in conventional III-V semiconductor 2DESs is not present.

Magnetization experiments were performed on three samples from two different MgZnO/ZnO heterostructures. Details of the sample preparation can be found in Refs. [21,22]. We focus here on the sample which exhibited the largest signals. Results obtained on the second sample from the same heterostructure are shown in the Supplemental Material [21]. The results on the sample from a different heterostructure are consistent with the results presented here. The electron density $n_s = 1.7 \times 10^{11} \text{ cm}^{-2}$ and mobility $\mu = 380\,000 \text{ cm}^2/\text{Vs}$ were determined from Shubnikov-de Haas and Hall effect measurements on a reference 2DES at 0.5 K [21]. r_s given by $m^*e^2/(4\pi\epsilon_0\epsilon_r\hbar^2\sqrt{\pi n_s})$, amounted to 9.0, where e denotes the elementary charge, ϵ_0 the vacuum permittivity, $m^* = 0.31 m_e$ the effective mass (m_e is the free electron mass), and $\epsilon_r = 8.5$ the dielectric constant of ZnO [23]. The area A of the studied 2DES was $0.9 \times 1.8 \text{ mm}^2$. We employed a calibrated micromechanical cantilever magnetometer to measure the

*mwilde@ph.tum.de

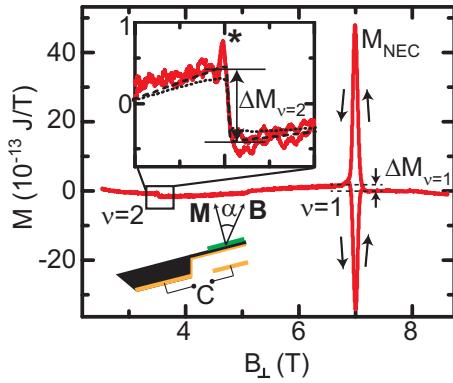


FIG. 1. (Color online) Oscillatory part of the magnetization of a MgZnO/ZnO heterostructure at $\alpha = 52.0^\circ$ and $T = 0.28$ K. At filling factor $\nu = 1$, the data exhibits the dHvA effect as well as large NECs, which change sign upon changing the sweep direction (arrows). In the inset, experimental data (light line) as well as model calculations [21] for the ideal (dashed line) and real (dotted line) 2DES are shown ($3.0 < B_\perp < 4.0$ T).

anisotropic magnetization M of the 2DES [21,24]. A capacitive readout scheme was applied to monitor the deflection of the cantilever beam [25] as depicted schematically in the inset of Fig. 1. The capacitance change provided the torque $\tau = \mathbf{M} \times \mathbf{B}$. From $\tau/(B \sin \alpha)$ we extracted the magnetization M assuming \mathbf{M} to be perpendicular to the plane given by the 2DES. The energy spectrum of an ideal 2DES is composed of discrete levels $E_{j,s} = (j + 1/2)\hbar\omega_c + sg\mu_B B$ with the cyclotron frequency $\omega_c = eB_\perp/m^*$ ($B_\perp = B \cos \alpha$ denotes the perpendicular magnetic field component), $s = \pm 1/2$, and the Landé factor g . $M(B)$ of an ideal 2DES exhibits steps of height $\Delta M/N = \Delta M/(n_s A) = \Delta E/B$ when the Fermi energy crosses an energy gap ΔE between two adjacent energy levels at integer ν [13,26]. ΔM_ν is a measure of the so-called thermodynamic energy gap ΔE at ν and thereby provides direct information about the DOS and possible many body effects [27]. We performed the measurements in a ^3He cryostat at temperatures down to 0.28 K. The experiments were conducted in a vector magnet system allowing magnetic fields up to 9 T under different angles $36.8^\circ < \alpha < 67^\circ$ in the same cool-down cycle. In an axial magnet, we performed further measurements at two fixed angles $\alpha = 36.8^\circ$ and $\alpha = 52^\circ$ up to $B = 14$ T. To analyze the data we performed model calculations considering a single particle DOS [25] as detailed in [21].

The magnetization of the MgZnO/ZnO heterostructure at $T = 0.28$ K for $\alpha = 52^\circ$ is displayed in Fig. 1. A smoothly-varying magnetic background signal has been removed from the raw data by subtracting a low-order polynomial fit in B . $M(B_\perp)$ exhibits the dHvA effect as jumps ΔM in the magnetization occur for $\nu = 2$ at $B_\perp \approx 3.5$ T (inset) and $\nu = 1$ at $B_\perp \approx 7$ T. Superimposed at $\nu = 1$ is a nonequilibrium (neq) signal M_{NEC} arising from NECs [28] showing the characteristic sign change upon changing the magnetic field sweep direction [15,29,30]. Contrary to $\nu = 1$, the signal near $\nu = 2$ does not contain sweep-direction dependent contributions indicating that both the step ΔM and the spike

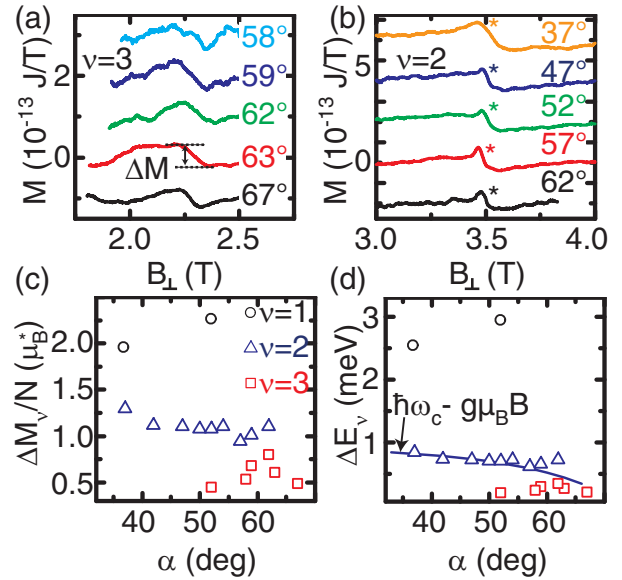


FIG. 2. (Color online) Angular dependencies of $M(B)$ near (a) $\nu = 3$ and (b) $\nu = 2$. Curves are shifted in the vertical direction for clarity. (c) dHvA amplitudes per electron $\Delta M_{e,\nu} = \Delta M_\nu/N$ as a function of α . Values for $\nu = 1$ were extracted from curves shown in Figs. 1 and 3(a). (d) Thermodynamic energy gaps ΔE_ν as a function of α . The line denotes the energy gap expected for $\nu = 2$ in a disorder-free 2DES at $T = 0$.

(marked by an asterisk in the inset) reflect equilibrium (eq) properties.

In Figs. 2(a) and 2(b) we depict angular dependencies of the dHvA effect for filling factors $\nu = 3$ and $\nu = 2$, respectively. In Fig. 2(c) we summarize $\Delta M_{e,\nu} = \Delta M_\nu/N$ for $\nu = 1$ to 3 taken at different α . First we discuss $\nu = 2$ where spin polarization of the 2DES is absent. $\Delta M_{e,\nu=2}$ ranges from 1.3 to $0.85\mu_B^*$ in the angular regime from $\alpha = 36.8^\circ$ to 62.0° . Here, $\mu_B^* = \mu_B(m_e/m^*)$ with $m^* = 0.31(\pm 0.01)m_e$ as determined from a Lifshitz-Kosevich analysis [11] of $\Delta M(T)$ at $\nu = 2$ (not shown). m^* is consistent with Refs. [5,8]. The corresponding energy gaps $\Delta E_\nu = M_{e,\nu} B_\perp$ are shown in Fig. 2(d). For an ideal (disorder-free) noninteracting 2DES one would expect the energy gap for $\nu = 2$ to amount to $\Delta E_{\nu=2} = \hbar\omega_c - g\mu_B B$ as denoted by the line in Fig. 2(d) ($g = 1.93$ is the band structure Landé factor [31]). The experimentally determined values of $\Delta E_{\nu=2}$ (triangles) are in good quantitative agreement with the prediction for the ideal 2DES.¹ This agreement is surprising as the finite mobility μ of the 2DES indicates residual disorder in the MgZnO/ZnO heterostructure. To further analyze the observed ΔM we show the dHvA amplitude calculated for the DOS of the real 2DES considering a finite energy level broadening $\Gamma = 5 \times 10^{-2} \sqrt{B_\perp}$ meV $T^{-1/2}$ [21] in the inset of Fig. 1 as a dotted line. The value expected from this is indeed smaller than the measured one, indicating that electron-electron interaction enhances the

¹Earlier transport experiments on MgZnO/ZnO heterostructures revealed coincidence phenomena in tilted magnetic fields [8,9]. At $\nu = 2$, the first coincidence is expected at $\alpha = 72.6^\circ$, i.e., beyond the upper limit of the x axis in Fig. 2(d).

dHvA amplitude in the MgZnO/ZnO heterostructure [13]. The dashed line in the inset shows $M(B)$ for the ideal 2DES at $T = 0$ K. The experimental curve closely follows this behavior indicating the already excellent quality of the 2DES [26,32]. However, there is an additional spikelike feature (asterisk) close to the steep slope. This feature will be discussed later.

We now consider the peak-to-peak amplitudes ΔM of the odd filling factors $\nu = 1$ and $\nu = 3$ where the Fermi energy resides in the Zeeman energy gap and spin polarization of the 2DES occurs. We find that $\Delta M_{e,\nu=3}$ varies with α taking a maximum value of $0.68\mu_B^*$. $\Delta M_{e,\nu=1}$ is considerably larger and amounts to a value of up to $\approx 2.25\mu_B^*$.

From the energy gaps of the odd filling factors $\nu = 3$ and $\nu = 1$, we extract the Zeeman spin splitting $\Delta E_Z = |g^*| \mu_B B$. In case of small disorder, spin splitting is known to be enhanced when approaching the quantum limit, i.e., in large fields B . This phenomenon is commonly attributed to the exchange interaction E_{Ex} [13] and expressed in terms of an effective factor g^* [33] as

$$\Delta E_Z = |g| \mu_B B + E_{Ex} = |g^*| \mu_B B. \quad (1)$$

From the data shown in Fig. 2(d) we extract a maximum $g^* = 1.1$ for $\nu = 3$. This value is reduced compared with the band structure g factor of ZnO. We attribute the reduction of g^* to the level broadening and in particular level overlap in the low field regime. For $\nu = 1$, we find a maximum g^* of 5.1 at $\alpha = 36.8$ deg. This value is significantly enhanced over $g = 1.93$.² Our dHvA experiment thus substantiates that electron-electron interaction plays an important role in the magnetic field dependent ground state properties of the MgZnO/ZnO heterostructure at both an even and odd integer ν .

Figures 3(a) and 3(b) shows the T dependence of $M(B)$ near $\nu = 1$ and $\nu = 2$, respectively, in the temperature range 0.28 to 1.6 K. For $T \leq 0.9$ K, there is a large signal arising from NECs superimposed on the dHvA signal at $\nu = 1$. The peak value of the NEC decreases with increasing T as has been reported for GaAs/AlGaAs heterostructures [28]. Here, we focus on the field position of the NEC maxima. At this position, the Fermi energy resides in localized states and the QHE edge channels are most strongly decoupled from the bulk, resulting in an effective suppression of backscattering. NECs are a very sensitive gauge for this effect, since the breakdown-limited NEC signal increases strongly for increasing suppression of backscattering. This is in contrast to magnetotransport experiments, where ρ_{xx} and ρ_{xy} exhibit zero and constant plateau values, respectively. Interestingly we find that the T -dependent maximum NEC value shifts towards smaller magnetic field values with increasing T . The shift of the NECs is highlighted for $\nu = 1$ in Fig. 3(c) where we plot the relative separation $\Delta B_{\text{neq}}/B_{\nu=1}$ between peaks at low T and the peak at $T = 0.9$ K (squares). The peak position varies almost linearly with T (line). Following Ref. [5] we exclude that the observed shifts arise from T -dependent variations in n_s as they set in only for $T > 1$ K. For $\nu = 2$ [Fig. 3(b)],

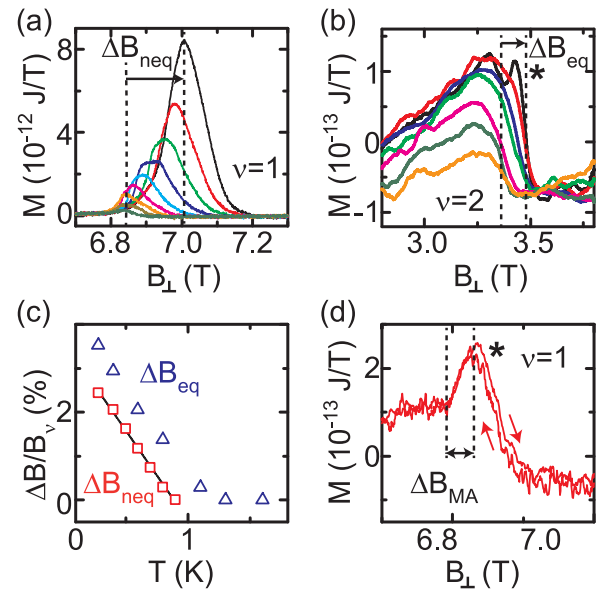


FIG. 3. (Color online) Temperature dependence of $M(B)$ near (a) $\nu = 1$ at $\alpha = 36.8^\circ$ and (b) $\nu = 2$ at $\alpha = 62.0^\circ$ measured for down-sweeping B . From top to bottom the temperature varies from $T = 0.28$ to 1.6 K. For $T \leq 0.9$ K NECs are present at $\nu = 1$ in (a). Going from higher to lower temperatures, the field position of the maximum nonequilibrium signal in (a) moves to larger B by ΔB_{neq} . A shift ΔB_{eq} is seen also for the equilibrium signal in (b). (c) $\Delta B_{\text{neq}}/B_{\nu=1}$ (squares) and $\Delta B_{\text{eq}}/B_{\nu=2}$ (triangles) as a function of T . At low T , ΔB_{neq} increases linearly with decreasing T as indicated by a linear fit (black line). (d) Spikelike equilibrium overshoot of $M(B)$ at $\nu = 1$ and $T = 1.6$ K.

we do not observe NECs in the temperature regime studied. However, we find a shift of the equilibrium dHvA oscillation to smaller B for increasing T . The relative shift $\Delta B_{\text{eq}}/B_{\nu=2}$ is displayed in Fig. 3(c). Below ~ 1 K, it also increases linearly as T decreases.

We now discuss the T -dependent shifts of nonequilibrium and equilibrium features. As mentioned above, the field position of the maximum NEC is directly connected to the minimum of ρ_{xx} [30]. Our data suggest that the minima of ρ_{xx} shift towards higher magnetic fields with decreasing T . Also the field position of the dHvA oscillation at $\nu = 2$ shifts by ΔB_{eq} as a function of T . The relative shift of both, ΔB_{neq} and ΔB_{eq} , is consistent in temperature and we thus suppose that they have the same microscopic origin. For an equilibrium property such as the dHvA effect, no T -dependent shifts have been reported before. Concerning nonequilibrium properties, displacements and asymmetries of QHE plateaus and corresponding ρ_{xx} minima have been observed in transport measurements on GaAs-based heterostructures [16,17,19]. They were attributed to scattering centers being present in the immediate vicinity of the 2DES. Repulsive scattering centers altered the DOS in such a way that it was asymmetric exhibiting an impurity tail at its high energy side [18], while attractive scatterers led to the opposite asymmetry [19]. As a consequence, localized states of the lower energy level and extended states of the next higher energy level in the DOS could overlap resulting in a shift of the ρ_{xx} minima towards higher B for repulsive scatterers. We find

²In Ref. [9], $g^* = 7.28$ was reported when addressing excited states in a transport experiment.

corresponding displacements in transport measurements on a reference sample [21]. From the direction of the observed shift in field position we infer that the interaction of charge carriers and scatterers in the MgZnO/ZnO heterostructure is repulsive.

We further observed spikelike overshoots of the equilibrium magnetization as depicted in the inset of Fig. 1, in Fig. 2(b), and in Fig. 3(b) (marked by the asterisks) for $\nu = 2$ at 0.28 K. At $\nu = 1$, we also observe an overshoot [Fig. 3(d)] at $T = 1.6$ K, where NECs are absent.³ The overshoots do not depend on the field sweep direction. Similar effects were reported for a bilayered 2DES in GaAs/AlGaAs [34]. The authors speculated that correlations effects or a peculiar form of the DOS was responsible for the overshoot. In the light of the fact of an asymmetric DOS we attribute this feature to magnetic thaw down of electrons [20]. In the presence of repulsive scatterers in close vicinity to the 2DES, localized magnetoacceptor states can exist at energies above the extended Landau states [20]. When electrons are transferred from the higher-lying localized to the lower-lying extended states, the free energy F of the electron system decreases. Correspondingly, there is an increase in $M = -\frac{\partial F}{\partial B}$ enhancing the equilibrium dHvA amplitude with a spikelike overshoot in the magnetic thaw down process near an integer ν . We apply the formalism of Ref. [26] and estimate the average density of magnetoacceptors

by $n_{\text{MA}} = n_s \Delta B_{\text{MA}} / B_{\text{av}}$, where ΔB_{MA} is defined in Fig. 3(d). B_{av} is the mean field value. We get $n_{\text{MA}} \approx 10^9 \text{ cm}^{-2}$. Magnetization measurements offer thus a tool to determine the nature and number of scatterers and thereby to get detailed insight into the microscopic sample structure. One might speculate that Zn vacancies at the interface [35] possibly act as the source of the repulsive scattering.

In summary, we studied electron-electron interaction and disorder effects in MgZnO/ZnO by means of the dHvA effect and NECs. The energy gaps at $\nu = 2$ and $\nu = 1$ were enhanced over the values expected in the single particle picture. Temperature dependent shifts of the filling factors and of the maxima of the NECs were found indicating the presence of repulsive scattering centers in the direct vicinity of the 2DES that forms at the interface without any intentional remote or short range doping. A method to determine their density from $M(B)$ was introduced. The shape of the dHvA oscillations was consistent with magnetic thaw down from magnetoacceptor states enhancing the quantum oscillatory magnetization even further beyond the electron-electron interaction. The results are important to further optimize MgZnO/ZnO 2DESs that potentially allow one to overcome mobility-limiting remote-donor scattering discussed for GaAs-based heterostructures.

We acknowledge financial support from the Deutsche Forschungsgemeinschaft via TRR80. This work was partly supported by Grant-in-Aids for Scientific Research (S) No. 24226002 from MEXT, Japan, as well as by the Murata Science Foundation (Y.K.).

³Here, the small remaining hysteresis is attributed to the self-induction of the superconducting magnet and the finite averaging time for data acquisition.

-
- [1] A. Ohtomo and H. Hwang, *Nature (London)* **427**, 423 (2004).
 [2] H. Y. Hwang, Y. Iwasa, M. Kawasaki, B. Keimer, N. Nagaosa, and Y. Tokura, *Nat. Mater.* **11**, 103 (2012).
 [3] N. Reyren, S. Thiel, A. D. Caviglia, L. F. Kourkoutis, G. Hammerl, C. Richter, C. W. Schneider, T. Kopp, A.-S. Retschi, D. Jaccard, M. Gabay, D. A. Muller, J.-M. Triscone, and J. Mannhart, *Science* **317**, 1196 (2007).
 [4] J. Bert, B. Kalisky, C. Bell, M. Kim, Y. Hikita, H. Hwang, and K. A. Moler, *Nat. Phys.* **7**, 767 (2011).
 [5] A. Tsukazaki, A. Ohtomo, T. Kita, Y. Ohno, H. Ohno, and M. Kawasaki, *Science* **315**, 1388 (2007).
 [6] A. Tsukazaki, S. Akasaka, K. Nakahara, Y. Ohno, H. Ohno, D. Maryenko, A. Ohtomo, and M. Kawasaki, *Nat. Mater.* **9**, 889 (2010).
 [7] P. Fulde, *Correlated Electrons in Quantum Matter* (World Scientific, Singapore, 2012).
 [8] A. Tsukazaki, A. Ohtomo, M. Kawasaki, S. Akasaka, H. Yuji, K. Tamura, K. Nakahara, T. Tanabe, A. Kamisawa, T. Gokmen, J. Shabani, and M. Shayegan, *Phys. Rev. B* **78**, 233308 (2008).
 [9] Y. Kozuka, A. Tsukazaki, D. Maryenko, J. Falson, C. Bell, M. Kim, Y. Hikita, H. Y. Hwang, and M. Kawasaki, *Phys. Rev. B* **85**, 075302 (2012).
 [10] C. Kittel, *Introduction to Solid State Physics* (Oldenbourg Verlag, Munich, 1993).
 [11] D. Shoenberg, *Magnetic Oscillations in Metals* (Cambridge University Press, Cambridge, 1984).
 [12] J. P. Eisenstein, H. L. Stormer, V. Narayanamurti, A. Y. Cho, A. C. Gossard, and C. W. Tu, *Phys. Rev. Lett.* **55**, 875 (1985).
 [13] A. H. MacDonald, H. C. A. Oji, and K. L. Liu, *Phys. Rev. B* **34**, 2681 (1986).
 [14] J. Eisenstein, H. Stormer, V. Narayanamurti, and A. Gossard, *Superlattices Microstruct.* **1**, 11 (1985).
 [15] A. Usher and M. Elliott, *J. Phys.: Condens. Matter* **21**, 103202 (2009).
 [16] J. E. Furneaux and T. L. Reinecke, *Phys. Rev. B* **33**, 6897 (1986).
 [17] R. J. Haug, R. R. Gerhardts, K. v. Klitzing, and K. Ploog, *Phys. Rev. Lett.* **59**, 1349 (1987).
 [18] S. Bonifacie, C. Chaubet, B. Jouault, and A. Raymond, *Phys. Rev. B* **74**, 245303 (2006).
 [19] A. Raymond, I. Bisotto, Y. M. Meziani, S. Bonifacie, C. Chaubet, A. Cavanna, and J. C. Harmand, *Phys. Rev. B* **80**, 195316 (2009).
 [20] I. Bisotto, C. Chaubet, A. Raymond, J. C. Harmand, M. Kubisa, and W. Zawadzki, *Phys. Rev. B* **86**, 085321 (2012).
 [21] See Supplemental Material at <http://link.aps.org/supplemental/10.1103/PhysRevB.89.075307> for additional information.
 [22] J. Falson, D. Maryenko, Y. Kozuka, A. Tsukazaki, and M. Kawasaki, *Appl. Phys. Express* **4**, 091101 (2011).
 [23] D. Maryenko, J. Falson, Y. Kozuka, A. Tsukazaki, M. Onoda, H. Aoki, and M. Kawasaki, *Phys. Rev. Lett.* **108**, 186803 (2012).

- [24] M. P. Schwarz, D. Grundler, I. Meinel, C. Heyn, and D. Heitmann, *Appl. Phys. Lett.* **76**, 3564 (2000).
- [25] M. A. Wilde, J. I. Springborn, O. Roesler, N. Ruhe, M. P. Schwarz, D. Heitmann, and D. Grundler, *Phys. Status Solidi B* **245**, 344 (2008).
- [26] S. A. J. Wieggers, M. Specht, L. P. Lévy, M. Y. Simmons, D. A. Ritchie, A. Cavanna, B. Etienne, G. Martinez, and P. Wyder, *Phys. Rev. Lett.* **79**, 3238 (1997).
- [27] A. Wasserman and M. Springford, *Adv. Phys.* **45**, 471 (1996).
- [28] C. Jones, A. Usher, M. Elliott, W. Herrenden-Harker, A. Potts, R. Shepherd, T. Cheng, and C. Foxon, *Solid State Commun.* **95**, 409 (1995).
- [29] M. P. Schwarz, D. Grundler, C. Heyn, D. Heitmann, D. Reuter, and A. Wieck, *Phys. Rev. B* **68**, 245315 (2003).
- [30] N. Ruhe, G. Stracke, C. Heyn, D. Heitmann, H. Hardtdegen, T. Schäpers, B. Rupperecht, M. A. Wilde, and D. Grundler, *Phys. Rev. B* **80**, 115336 (2009).
- [31] H. Tampo, H. Shibata, K. Maejima, A. Yamada, K. Matsubara, P. Fons, S. Kashiwaya, S. Niki, Y. Chiba, T. Wakamatsu, and H. Kanie, *Appl. Phys. Lett.* **93**, 202104 (2008).
- [32] M. A. Wilde, M. P. Schwarz, C. Heyn, D. Heitmann, D. Grundler, D. Reuter, and A. D. Wieck, *Phys. Rev. B* **73**, 125325 (2006).
- [33] T. Englert, D. Tsui, A. Gossard, and C. Uihlein, *Surf. Sci.* **113**, 295 (1982).
- [34] I. M. A. Bominaar-Silkens, M. R. Schaapman, U. Zeitler, P. C. M. Christianen, J. C. Maan, D. Reuter, A. D. Wieck, D. Schuh, and M. Bichler, *New J. Phys.* **8**, 315 (2006).
- [35] A. Uedono, T. Koida, A. Tsukazaki, M. Kawasaki, Z. Q. Chen, S. Chichibu, and H. Koinuma, *J. Appl. Phys.* **93**, 2481 (2003).